This paper addresses the issues relating to the use of 3-D printing tools in order to manufacture the structural elements of machines and apparatuses. The features of printing with the application of PLA-Carbon and PEEK (PEEK-Carbon) plastics have been analyzed. It is shown that printing that employs PEEK-plastic is accompanied by a series of problems associated with the high residual thermal stresses at cooling the material, as well as with the issue of adhesion to the laying surface, which should maintain its properties to a temperature of 420 °C. The causes of defects in the printing of articles with a significant process duration (longer than 12 hours) have been analyzed. It is shown that the most acute problem has been the interlayer grip, which predetermines the anisotropy of the properties of the finished product.

It has been proven that the use of PEEK plastic makes it possible to produce force elements by applying special print heads. Particular attention should be paid to the reliable connection between a printed element and the base (table) because the peeling and deformation of the base surface are one of the main causes of geometric defects, which subsequently predetermine the structural defects.

Mechanical tests of finished products have been performed, including vacuum and degassing research. It is established that the destruction of samples, in general, corresponds to classical ideas about the destruction of a quasi-fragile body when it comes to the phenomena occurring in the plane of the material's layers. Thus, any form printed by a printer is an orthotropic article whose behavior is satisfactorily described by Griffiths theory. At the same time, the strength characteristics, as well as elastic properties of a product demonstrate significant axial (orthotropic) differences.

It is also shown that the functional properties of a product are ensured by the comprehensive dynamic-moving and thermobaric influence on the melt of the material in the space behind a nozzle owing to which the planes of adhesion and hollowness of the finished product are formed.

The recommendations have been formulated for preventing defects and the elimination of delamination phenomena, errors in the geometric parameters of a product; it has been concluded that it is appropriate to implement these processes into production

Keywords: 3-D printing, additive processes, PEEK filament, extrusion, vacuum research, mechanical testing

UDC 621.45.778
DOI: 10.15587/1729-4061.2020.211752

ENSURING THE FUNCTIONAL PROPERTIES OF RESPONSIBLE STRUCTURAL PLASTIC ELEMENTS BY MEANS OF 3-D PRINTING

A. Salenko
Doctor of Technical Sciences, Professor
Department of Design of Machine Tools and Machines
National Technical University of Ukraine
«Igor Sikorsky Kyiv Polytechnic Institute»
Peremohy ave., 37, Kyiv, Ukraine, 03056
E-mail: salenko2006@ukr.net

P. Melnychuk
Doctor of Technical Sciences, Professor
Department of Applied Mechanics
and Computer-Integrated Technologies
Zhytomyr Polytechnic State University
Chudnivska str., 103, Zhytomyr, Ukraine, 10005
E-mail: meln_pp@ukr.net

E. Lashko
PhD, Assistant*
E-mail: evgeny.lashko.lj@gmail.com

O. Chencheva
PhD, Assistant*
E-mail: chenchevaolga@gmail.com

O. Titarenko
Postgraduate Student*
E-mail: titarenko_om@protonmail.com

I. Derevianko
Engineer of Laboratory**
E-mail: derevianko_ii@protonmail.com

O. Samusenko
Head of Laboratory**
E-mail: samusenko_oa@protonmail.com
*Department of Industrial Engineering
Kremenchuk Mykhailo Ostrohradskyi National University
Pershotravneva str., 20, Kremenchuk, Ukraine, 39600
**Yuzhnoye State Design Office
Kryvorizka str., 3, Dnipro, Ukraine, 49008

Received date 20.03.2020
Accepted date 10.09.2020
Published date 13.10.2020

1. Introduction

Recently, there has been active development of scientific research aimed at the manufacture of various parts and their prototypes by means of 3-D printing. The additive technologies used typically imply the point, continuous-linear, or layered application of a material onto a flat base, owing to which the formation of the object is carried out in stages, layer

by layer until the specified shape is fully reproduced. The objects themselves are made both from polymers (originally supplied in the form of filaments or photopolymer resins) and metals (powders of different dispersity and composition).

Typically, researchers focus mainly on the accuracy of reproducing the shape of the product, neglecting other functional properties of the product. Among the latter, for responsible elements and parts, the most relevant parameters are strength, hardness, and for individual products – density, hollowness, and gas permeability. It is obvious that these functional properties should be provided, in accordance with the technical requirements, by special printing procedures, the modes and technique of laying an extruded material, as well as the application of a particular material used.

The lack of systematized information on the conditions and features of the formation of the structure of printed products, the formation of adhesive areas on the contact planes of the embedded layers, structural features, hinders the implementation of FDM processes and narrows the scope of their application. At the same time, there are now a large number of new types of plastics, various composites, which are also used for the formation of products in traditional ways.

Therefore, studies aimed at describing the phenomena and establishing patterns in the formation of the structure and functional properties of the product received by an FDM method are relevant and can expand the scope of this process application. At the same time, this could provide a scientific basis for improving the method and for further optimization studies of the process in order to adapt it for engineering practice.

2. Literature review and problem statement

Currently, there are many studies tackling the possibilities of additive technologies, the prospects of using them in various fields, including biology, surgery, construction, etc. Almost all these processes are based on the main principle of product formation: a single layer of the surface is formed from the prepared material by extrusion (FDM-process), surface melt (LS), or photochemical conversion. Thus, work [1] notes that the FDM process is the simplest; its implementation employs a plastic thread blank (filament), which melts in the extruder and then mechanically extruded to the surface of the base. However, the unresolved issues are related to overcoming existing restrictions on materials. Papers [2, 3] report the results of studying many modern 3-D printers for both professional and household use, which differ primarily in layout and service functions. However, the authors were unable to summarize patterns regarding the type of machines and equipment for 3-D printing and the relevant materials that should be used in each type of machine.

The printers forming a layer by laser baking are described in work [4]; they, however, have a small working area, and a significant price, because they use special optical systems, a laser head, expensive photopolymer resins. All this imposes restrictions on the use of the LS process for the manufacture of high-precision models, particularly in the aerospace industry. The dimensions of the work tables range from 60×60 mm to 200×200 mm but the high price and insufficiency of the product range of photopolymer resins do not make it possible to actively exploit such printers to solve industrial tasks.

Laser baking printers are industrial equipment, as shown in [4, 5], which causes objective difficulties related to the needs of special premises, communications, appropriate electrical power, etc. For baking, powders of different metals are used; the resulting quality is comparable to the quality of layers after semi-finished machining, the accuracy of the model reproduction is not worse than IT9...10, resolution – up to 0.05 mm.

The option of overcoming the appropriate difficulties may be the FDM process, given that modern production is increasingly focused on the use of plastic masses, which is the focus of paper [6]. In this case, the authors consider only ABS-plastic, not including new materials that would have better physical and mechanical properties, resistance to aggressive environments, endurance to cyclical and sign-changing loads, etc. In part, this flaw is corrected in study [7], in which the authors analyze the strength indicators of materials for printing in their original state (in the form of a filament) and after extrusion. In this case, the authors of work [8] report the results of studying reinforced materials strengthened with fibers. Such materials have greater resistance to damage; however, the unresolved issues are related to the use of polylactide filament reinforced with impregnated carbon fiber.

It should be noted that conventionally common printer layouts, the printing heads and polymeric materials used are mainly aimed at creating models with the accuracy of rendering sizes according to IT 10–12. At the same time, the printing of parts capable of bearing certain technological loads is complicated. This situation predetermines the expediency of research on finding new printing techniques based on the analysis of phenomena that occur both in the extruder and at the time of laying out the melt on the work surface.

3. The aim and objectives of the study

The aim of this study is to ensure the functional properties of elements and products received through the FDM processes based on establishing patterns that predetermine the output parameters by the conditions and modes of printing. This would make it possible to define the rational techniques and methods for reproducing responsible products using printers with the conventional arrangement.

To achieve the set aim, the following tasks have been solved:

– to analyze, based on the typical structure of a force element, the conditions of polymer composite laying out and to establish the conditionality of the output parameters of accuracy and roughness on the laying out conditions;

– to examine the process of extruding the material and establish the effect of extrusion conditions on the strength characteristics of the finished product, the anisotropy of its properties;

– to evaluate the gas permeability of products, as well as the conditionality of this parameter by printing conditions.

4. Research methods and applied materials

In this research, the analytical methods were used for predicting the stressed state of elements [9] made by 3-D printing means. We have estimated the impact of cracks and delamination, formed during the laying out of the filament, on the strength characteristics of the product; the mechanical, thermal, and vacuum tests of finished products were carried out.

As an object to print, a flange of the fuel tank was chosen (Fig. 1, *b*), received by the winding the carbon fibers on the liner with the installation of two such flanges.

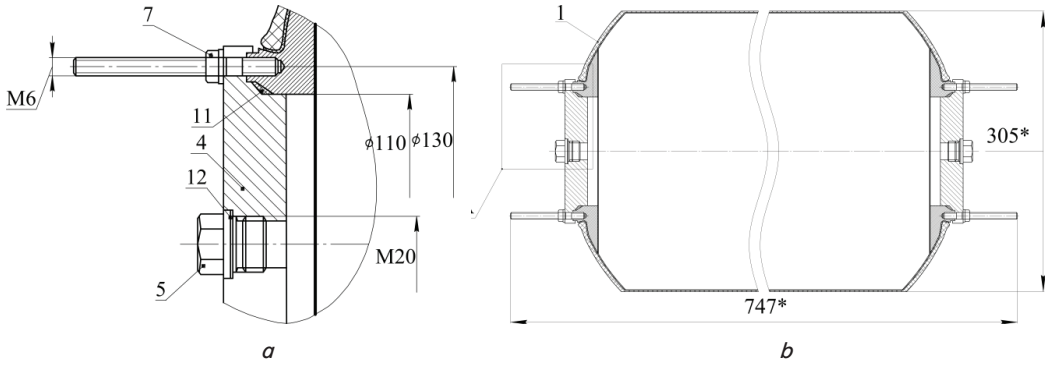

Fig. 1. Finished product: *a* — a flange with a lid installed in the product; *b* — fuel tank

A flange is installed in a carbon tank with its subsequent gluing to the wound outer shell (Fig. 1, *a*). Installing in the tank proceeds until the winding moment (laying a prepreg), before the impregnation and polymerization of the tank shell in general.

Delta-type printers were used, with a working area size of 290×290×260 mm, as well as the port-type printers. with a working area size of 200×200×150 mm. A first printer was equipped with a Bowden-head, that is, with the filament supply tool separate from the heating part of the extruder; this printer was used to print with the application of PLA-Carbon plastic (extrusion temperature, 260–265 °C). A second printer (Fig. 2, *a*) was equipped with a high-temperature head with liquid cooling to operate with PEEC plastic (melting point, 420–430 °C).

The head was made independently (Fig. 2, *b*); the extrusion process was controlled by involving additional channels of the RUMBA control device.

Filaments of polylactide, reinforced with cut carbon fiber (PLA-Carbon), had the rated limit of the tensile strength of 55 MPa, PEEK-Carbon materials – 110 MPa.

Materials properties are given in Tables 1, 2.

Table 1

PLA-carbon material properties

Indicator	ASTM	Test conditions	Measuring unit	Typical value
Mechanical				
Tensile strength	D638	50 mm/min	MPa	56
Elongation	D638	50 mm/min	%	9
Flexible force	D790	2 mm/min	MPa	89
Bending module	D790	2 mm/min	MPa	2.570
Impact force, IZOD	D256	3.2 mm; 23 °C	kJ/m^2	3.4
Thermal				
Bending temperature under load	D648	0.45 MPa; 6.4 mm	°C	130–140
Other				
Melt flow rate	D1238	190 °C; 2.16 kg	g/10min	5
Specific weight	D792	23 °C	g/cm^3	1.282
Shrinkage	D955	23 °C	%	0.5

Table 2

Properties of PEEK plastics

Indicator	TECAPEEK (PEEK)	TECAPEEK HT (PEK)	TECAPEEK ST (PEKEKK)
T_g	150 °C	160 °C	165 °C
Density	1.31 g/cm^3	1.31 g/cm^3	1.32 g/cm^3
Elasticity module	4.200 MPa	4.600 MPa	4.600 MPa
Working temperature, const.	260 °C	260 °C	260 °C
Working temperature, instant.	300 °C	300 °C	300 °C
Minimal working temperature (disabling at *t* to –100 °C, increase in friability)	–40 °C	–40 °C	–40 °C

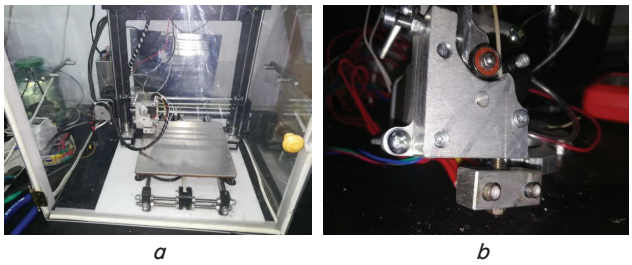

Fig. 2. Equipment used:
a — a 3-D printer; *b* — a high-temperature working head

Since strength, geometric accuracy, and gas permeability are most important among the properties of the product, the main attention during our study was focused on these characteristics.

Before work, the material was subjected to mechanical tests, micro electron testing, and weighing in order to determine its density (in the absence of moisture). Microelectron photography (×300), shown in Fig. 3, confirms the characteristics claimed by the manufacturer.

In addition, the filament was checked for defects in the form of formations of a larger or smaller (from 1.75 mm) diameter.

For the sealed test, round blanks with a diameter of 80.0±0.25 mm and a thickness of 4.8 mm and a flange were printed in accordance with the drawing by the customer. The filling density was 90 % for the core and 100 % for the

embedded thread on planes of 2.8 mm thick. The printed product was checked in a vacuum chamber with a change in the temperature of the study and in working conditions. To this end, the lid was fixed to a regular place, and the central hole was muffled with a cork. After installation, we received the structure, which was mounted on the bench to determine tightness.

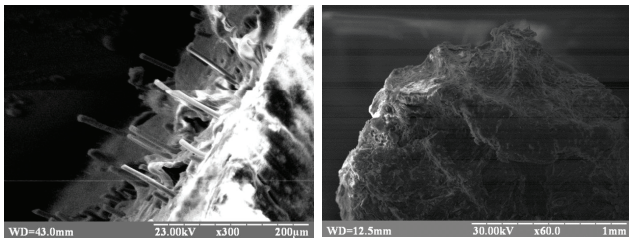

a *b*

Fig. 3. Microelectron image of the filament's end in the PLA-Carbon and PEEK plastics

For a more accurate quantitative assessment of the level of tightness of products, more accurate vacuum studies with appropriate metrological support are required.

The methodology for conducting tests was as follows. To quantify the tightness of the finished product, we considered the fact that the flow of current B is characterized by the amount of gas that penetrates through the leaks in a unit of time. Leaks are formed due to a violation of the density of layer layout, as well as due to the deformation of the product during workloads. The dependence takes the form of the product of volume V, occupied by gas, by the speed of change in pressure $\Delta P/\Delta t$ after the pumping stops:

$$B = \frac{V\Delta P}{\Delta t}. \quad (1)$$

The standard conditions for determining the current B [Pa·m^3/s] are: pressure difference between the inside and outer sides of the product ΔP=105 Pa, test gas – air (pure nitrogen was used in the study), temperature – 298 K.

The ratio of the flow rate of current B under standard conditions to the flow Q under arbitrary conditions in the viscosity mode of gas flow is expressed from the Poiseuille equation and takes the following form:

$$B = Q\frac{\eta_{gas}}{\eta_{air}}\frac{P_{atm}^2}{P_2^2 - P_1^2}, \quad (2)$$

where η_{air} is the coefficient of the dynamic viscosity of air, η_{gas} is the coefficient of the dynamic viscosity of test gas, P_2 and P_1 are the partial pressure of test gas from the outside and inside of the object, P_{atm} is atmospheric pressure.

For the molecular regime of the current, the ratio is determined from the ratio of molecular masses of gases and takes the following form:

$$B = Q\frac{M_{gas}}{M_{air}}\frac{P_{atm}}{P_2 - P_1}, \quad (3)$$

where M_{air} is the molecular mass of air, M_{gas} is the molecular mass of test gas.

To choose the character of gas leakage, the following general provisions are used: for a current whose flow is less than 10^{-8} Pa·m^3/s, there is a molecular mode of the current, exceeding 10^{-5} Pa·m^3/s – viscous. In the intermediate area, the mode is combined. Calculations in it are produced on the basis of both ratios with the subsequent choice of the prevailing flow current.

For the case of vacuum testing of the product installed in the tank, the time of change in the pressure Δt, pumped in the device, can be calculated from the following formula:

$$\Delta t = 2.3\frac{V}{S}\ln\left(\frac{P_{init}}{P_{perm}}\right), \quad (4)$$

where V is the volume of a pumped-out object (m^3), S is the effective pumping speed (m^3/s), P_{init} is the initial gas pressure in a product (Pa); P_{perm} is the permissible maximum gas pressure in a product (Pa).

When neglecting the flow of degassing from the walls and taking into consideration the assumption about the absolute tightness of the winding outer shell, the flow of gas through the open parts of the flange will be determined by the hollowness of the material and the formed through flows. The calculation involves the working gas that fills the sealed product during operation or storage. The maximum permissible current of flow Q for the working gas in the device will then be determined from the following ratio:

$$Q = 2.3P_{init}\frac{V}{S}\ln\left(\frac{P_{init}}{P_{perm}}\right). \quad (5)$$

To investigate the tightness of the samples of round shape, the universal vacuum post VUP-5 was used, having installed special technological equipment in the control window. The parameter of the current B was assessed by a change in pressure in the vacuum chamber, considering the external pressure to be constant and equal to 0.113 MPa. The residual pressure then is $P_{init}=10^{-3}$ Pa.

5. Results of studying the process of 3-D printing

5. 1. Analysis of the techniques for laying out a polymeric composite

The process of the layered laying of filament, regardless of the plastic used, implies that the melt is extracted from the nozzle and placed on the surface, forming a layer of the frozen material. In this case, the volume of squeezing, due to the speed of extrusion, the distance to the surface of the laying, determine the shape of the laid part of the melt, as well as the force of pressing to the surface [10, 11].

Since printing proceeds from the base plane of the surface, and the process itself is multifactorial and multi-stage, the effect on strength, as shown in [3, 10], is exerted by the following:

– the type of material (strength limit, relative elongation);

– the extrusion temperature T_e;

– he table temperature T_o (that also indirectly determines the internal stresses σ_c and τ);

– the extrusion coefficient k_e;

– the fill density k, k=1.0–0.99;

– the extruder's diameter d_e and the layer thickness t_s, t_s~0.2–0.3d_e.

The latter determines the achievable roughness Ra (Rz). For single horizontal layers, Ra~6.3–12.5 µm. For vertical surfaces, Rz 80–40 µm (possibly higher, up to 6.3 µm).

For the curved surfaces, *Rz* is 80 μm. The accuracy of dimension execution corresponds to the quality $\pm\frac{IT9}{2}$ (with appropriate configuration); however, more traditional is the quality $\pm\frac{IT11}{2}$. Temperature deformations for different materials are different, for PLA and ABS~1.5–1.25 %, PEEK-Carbon ~0.6–0.8 %. Deformations are compensated for by the appropriate adjustment. For the characteristics of strength, an important point is the laying of layers. It is necessary that the extrusion coefficient k_e, filling coefficient k, and the layer thickness t_s are synchronized. The error leads either to delamination or to a drop in adhesion.

The temperature and its stability $T_{ABS,\ PLA}$~30–245 °C (the onset of extrusion at T~370–380 °C).

Since the finished product must meet the strength requirements, as well as tightness in general, the printing was performed with a 100 % filling of surface layers and a 90 % filling of the core. Thus, we achieved a certain weight saving while maintaining mechanical characteristics and surface density.

An important point is the laying of the layers of a material, which can be linear or concentric (Fig. 4). Since the object is in the form of a flange, it was decided to work with the linear laying of layers.

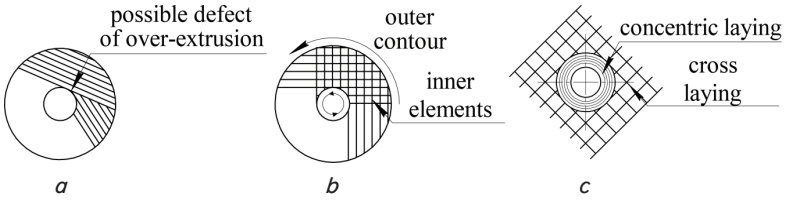

Fig. 4. Schematic laying of layers on the base plane

We laid the layers according to the classical scheme – by orthotropically extruded threads, with a layered build-up of thickness along the *z* coordinate. When bypassing the contour, we laid the thread along the tangent to the bending contour at a value of Δ=2.0 mm.

The stresses arising in places of the laying lead to the emergence of conditions for active crack formation on concentrators.

5. 2. Forecasting the strength of the product and conditions for the loss of operability

When calculating structures based on the yield strength σ_T or the strength limit σ_{mm}, it is accepted to use a material with the increased strength under a uniaxial load. However, experience shows that even the use of new high-strength materials does not rule out the possibility of a structure's failure due to its rapid macro-fragile destruction. Fragile destruction of the solid body occurs at relatively small plastic deformations, so the specific work carried out in the plastic flow of the material is close to zero:

$$W_p = \int_0^{\varepsilon_{ij}^{(p)}} \sigma_{ij} d\varepsilon_{ij}^{(p)} \approx 0. \quad (6)$$

Such destruction is characterized by the unstable propagation of a crack in the body of the material, that is, if the crack began to grow, the stress system contributes to its accelerated growth. It is this issue that causes debate since the materials used for printing cannot be considered quasi-fragile. The presence of a significant number of initial defects in the body of the material in the form of cavities between the stacked threads stimulates the weakening of the material while preceding the active growth of cracks and their transition into the critical ones.

Fragile destruction is considered from the positions of the mechanism of accumulation of damages and the propagation of cracks as a result of the transformation of the accumulated elastic energy of the deformed body. The process of destruction consists of two consecutive stages: the origin and growth of a crack. Obviously, the mechanism of fragile (quasi-fragile) destruction can be used to describe the phenomena of destruction regarding printed bodies.

It is known that the tension at the top of the crack, depending on the plastic properties of the environment, may equal the yield strength σ_T if the environment is plastic, or can be estimated by the value $K_\sigma\sigma$, if the environment is fragile (quasi-fragile). Here σ is the average stress applied at a distance from the crack; $K_\sigma \geq 1$ is the effective stress concentration factor.

The start of the destruction of structures is due to the high local stresses and deformations in places of the concentration of stresses. The required estimation dependences to quantify the stress-deformed state around different incisions were obtained for the static and quasi-static tasks of the linear elasticity theory for the case of small deformations.

Since when printing layers are stacked together with a possible small gap between two adjacent threads, the cavity of occurrence or spread of a crack can be conditionally selected in the form of an ellipse. It is known from [12] that the maximum stresses at the tops of an elliptical cut are determined from the following formula:

$$\sigma_y = \sigma\left(1+2\sqrt{\frac{l}{R}}\right), \quad (7)$$

where R is the curvature radius at the top of the main axis of the elliptical crack (Fig. 7).

If the defects are shaped like a sharp crack, then $R\to 0$ and $\sqrt{2l/R} \gg 1$, hence:

$$\sigma_y = 2\sigma\sqrt{\frac{l}{R}}. \quad (8)$$

For crystalline materials, the maximum stress at the top of the sharp crack will be:

$$\sigma_{\max} = \sigma_y = 2\sigma\sqrt{\frac{l}{R}}, \quad (9)$$

which makes it possible to determine the coefficient of stress concentration as:

$$K_\sigma = \frac{\sigma_{\max}}{\sigma} = 2\sqrt{\frac{l}{R}}. \quad (10)$$

For materials susceptible to stresses during printing, one can accept conditionally that $R=a_0$, where a_0 is the interatomic distance, and $\sigma_y=\sigma_{\max}$, but, for a polymer, destructive stress in the form of $\sigma=\sigma_f=\sqrt{\frac{E\gamma}{4l}}$, requires clarification of the γ coefficient value.

The presence of a crack in the body significantly changes its strained-deformed state and complicates the mathematical

notation. The same applies to the workpiece printed by laying out the fiber. However, since, according to [13], cracks are typically simulated by the ideal infinitely thin incisions, we shall reduce the problem of predicting the spread of cracks in the body to the problem in a classical statement.

The most problematic in terms of strength is the case of the delamination of the printed product (Fig. 5, *a*, *b*). In the case of flat deformation, the components of stresses and deformations near the crack [14, 15] are determined from the following formulae:

$$\sigma_x = \frac{K_I}{\sqrt{2\pi r}}\cos\frac{\theta}{2}\left(1-\sin\frac{\theta}{2}\sin\frac{3\theta}{2}\right);$$

$$\sigma_y = \frac{K_I}{\sqrt{2\pi r}}\cos\frac{\theta}{2}\left(1+\sin\frac{\theta}{2}\sin\frac{3\theta}{2}\right); \qquad (11)$$

$$\tau_{xy} = \frac{K_I}{\sqrt{2\pi r}}\cos\frac{\theta}{2}\sin\frac{\theta}{2}\cos\frac{3\theta}{2};$$

$$\sigma_z = V\left(\sigma_x+\sigma_y\right);$$

$$\tau_{xy} = \tau_{yz} = 0;$$

$$u_x = \frac{K_I}{G}\sqrt{\frac{r}{2\pi}}\cos\frac{\theta}{2}\left(1-2V+\sin^2\frac{\theta}{2}\right);$$

$$u_y = \frac{K_I}{G}\sqrt{\frac{r}{2\pi}}\sin\frac{\theta}{2}\left(1-2V-\cos^2\frac{\theta}{2}\right);$$

$$u_z = 0,$$

where K_I is the stress intensity factor;

$$K_I = \frac{1}{\sqrt{2\pi l}}\int_{-l}^{l}\sigma(\xi)\sqrt{\frac{l+\xi}{l-\xi}}\,d\xi. \qquad (12)$$

In the mechanics of destruction, stress intensity coefficients are one of the most important parameters that characterize the distribution of stresses near cracks in elastic bodies. They underlie the application of the principles of linear mechanics of destruction in the calculation of the strength and durability of structural elements [16, 17].

In formulae (12), at $y=0$, $x>0$:

$$\sigma_x = \sigma_y = \frac{K_I}{\sqrt{2\pi l}}, \quad \tau_{xy} = 0;$$

at $y=0$, $x<0$:

$$u_y = \frac{K_T}{G}(2-2V)\sqrt{\frac{r}{2\pi}}; \quad u_x = 0.$$

The flat-stressed state is determined as follows:

$$\sigma_z = 0; \quad u_z = \frac{V}{E}\int\left(\sigma_x+\sigma_y\right)dz. \qquad (13)$$

under condition $V = \frac{V}{1+V}$.

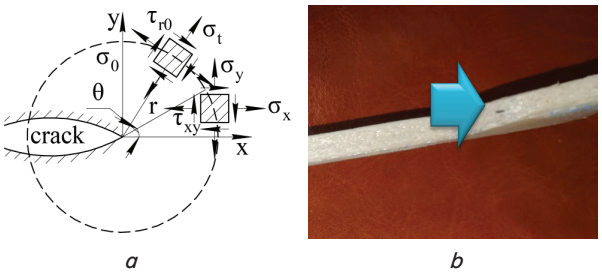

a *b*

Fig. 5. Delamination of a printed product: *a* — components of stresses and deformations under flat deformation; *b* — the photograph of a sample with a defect in the form of delamination

At fairly small $r>0$, these dependences can serve to assess the parameters of the stressed-deformed state around the banks of a crack.

We shall analyze the stress intensity factor K_I. Assume $\theta=0$ for a crack with the normal detachment. Then $\sigma_y\to\infty$ according to (7) at $r\to 0$. Such behavior of functions is termed a feature, and the K_I coefficient is the coefficient for a feature. Thus, in all ratios (12), the stresses have a feature of $1/\sqrt{r}$, the displacements – $\sqrt{r}$, that is, K_I, K_{II}, K_{III} are the coefficients for the features.

The criteria for assessing the limit state of cracks are based on the model of the ideal fragile body [18]. Local destruction at the top of the crack can transfer into involuntary one when a certain condition is met for energy reasons (according to Griffiths). Fragile destruction for the involuntary propagation of a single crack in a linearly elastic body would occur when, at a small elongation of the crack, more elastic energy is released than it is required for the specific energy of the formation of new crack surfaces.

If the elliptical cut in the elastic plane, which is evenly stretched to infinity by the stress σ, is replaced with an infinitely thin incision of length $2l$, the work of the stresses σ at the displacements u_y when uncovering the crack and when its banks are moved, is:

$$A = 2B\left(-\frac{1}{2}\sigma\int_{-l}^{l}u_y\,dx\right) = 2B\left(-\frac{1}{2}\sigma\int_{-l}^{l}2\sigma\frac{\sqrt{l^2-x^2}}{E}\,dx\right) =$$

$$= -\frac{2B\sigma^2}{E}\cdot\frac{1}{2}\left[x\sqrt{l^2-x^2}+l^2\arcsin\frac{x}{l}\right]_{-l}^{l} = \frac{\pi l^2\sigma^2}{E}B, \qquad (14)$$

where B is the width of the plate.

Magnitude A represents the work of crack disclosure. A change in the full elastic energy Δu_e of for a flat strained state is:

$$\Delta u_e = -\frac{\pi l^2\sigma^2}{E}B, \qquad (15)$$

and, for the flat deformation, is:

$$\Delta u_e = -\left(1-V^2\right)\frac{\pi l^2\sigma^2}{E}B. \qquad (16)$$

Then Griffith's criterion for a flat stressed state takes the form of $\sigma = \sqrt{\frac{2\gamma E}{\pi l}}$ and, for the flat deformation, is:

$$\sigma = \sqrt{\frac{2\gamma E}{\pi l\left(1-V^2\right)}}. \quad (17)$$

Ratio (17) is an expression for destructive load depending on the initial length of the crack and represents an achievement of the Griffiths theory. According to (11), the process is as follows: with the increase in load σ, the initial length of the crack does not change until σ reaches the boundary value σ_c.

Therefore, according to the above, it becomes clear that the reduction of the strength of the printed product will be caused not only by reducing the contact of adhesion but also by the manifestations of the phenomena of crack formation when certain critical stresses are achieved. These stresses are the greater the smaller the contact area between the layers.

Crack emergence places. Considering the product in the form of a flange (Fig. 1, *a*), note that the latter also includes integrated elements in the form of the molded nuts or bolts (Fig. 6). Such a molding is possible because the print head can form a cavity for the fastening element, which at a certain point in time will be integrated into the product. However, the problem of stresses and critical deformations gets much more complicated.

We have performed the solid-body modeling of the flange to obtain the layout by the means of 3-D printing and determine the stressed-deformed state of the product under the influence of loads. We have simulated the forces concentrated on the pins from the side of the lid and the action of pressure on the inner surface of the flange pen and the area with the formation of nuts. The load in the form of the pressure of 0.75 MPa was also applied to the neck of the flange, which simulates the effect of pressure from the inner cavity. The built solid-body model and the force load diagram are shown in Fig. 7, *a*, *b*. Calculations were performed in the Solid Works programming environment.

Under the influence of pressure, the product is in a three-dimensional stressed state; the corresponding diagrams of the resulting stresses and movements in the flange elements are shown in Fig. 8.

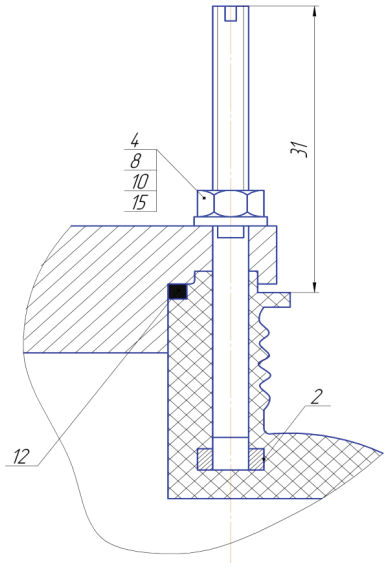

Fig. 6. Fragment of a flange structure with an embedded element in the form of nuts

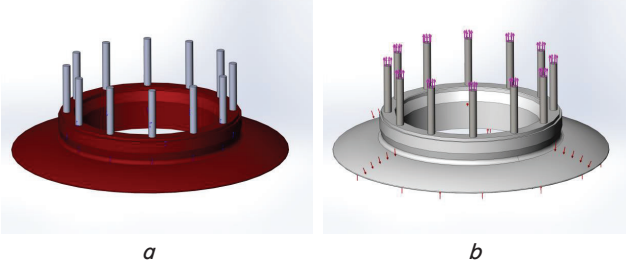

a *b*

Fig. 7. Solid-body modeling:
a — the built solid-body model of a flange with embedded elements; *b* — the force load applied to the base of the flange and to the fastening elements of the lid

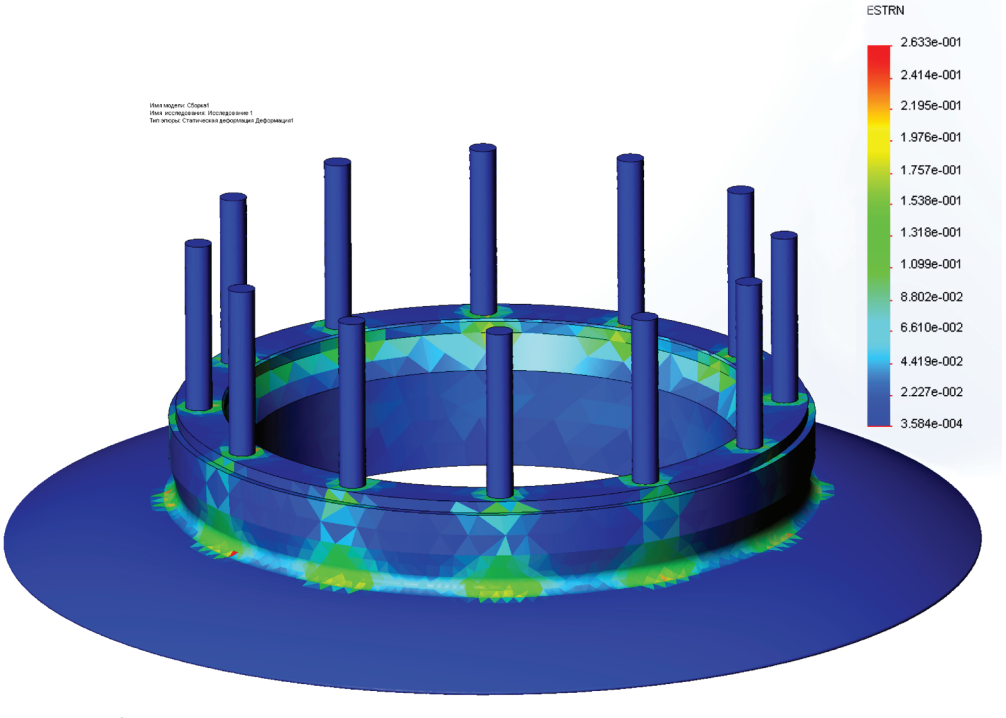

Fig. 8. Zones of maximum deformations arising in places of the embedded elements, as well as areas of the origin of radial cracks

It becomes obvious that the maximum displacements at the fixed upper plane are expected at the lower end; at the same time, the places of nuts laying, according to forecasts, may move from their positions, which would possibly cause the depressurization of the tank. In this case, a change in loading conditions significantly affects the emerging stresses and deformations.

Thus, based on the analytical analysis, it can be noted that the printed products will demonstrate a certain anisotropy of the properties due to the difference between the material's strength limit σ_b after laying on the base and the strength of the adhesion grip σ_a. The strength of the adhesive grip depends on the density of plastic laying (typically, a 100 % filling is rarely used and is associated with the complexities of accurate dosage of the material).

Our modeling of the behavior of the product has proven that the conditions of location of the embedded elements would play a significant role, while the load, with internal pressure, could cause the emergence, on the flange edge, of the radial areas of crack development and destruction of the product.

The cyclical and sign-change loading the products need clarification of the effect of the material's non-density on crack opening, and the temperature fields – on the residual thermal stresses arising between the layers.

6. Practical implementation of the FDM process of manufacturing responsible parts

After several unsuccessful attempts to perform the formation of simple objects (in the form of a sample plate for bend testing and a circle for testing the interlayer breakdown), the equipment was refined:

– a protective screen is made to stabilize the temperature on the work table, as well as to prevent chemical volatile compounds and evaporation from entering the workspace;

– an additional driver is installed for heating the table (with a separate power supply), which ensured the heating of the table within 110–120 °C;

– a separate driver is installed to heat the hot-end (two heaters with a total capacity of 250 W are applied) to an operating temperature of 420–435 °C.

The object to be formed is a composite blade for mechanical tests in accordance with DSTU. The thickness of the blade is $5.0_{-0.21}$ mm. The program was performed after the table's temperature reached 112 °C, the temperature in the extruder – 420–435 °C.

We have established the pattern of defect formation when printing with a PEEK material due to the detachment from the supporting platform. It is shown that the PEEK plastic can be satisfactorily printed only after careful removal of moisture from the surface of the monofilament, for example, in drying cabinets over 10–12 hours, and relative humidity in the room not exceeding 45 %.

The work area should be completely closed. Even a slight air movement causes perturbation when printing, which is manifested by the certain deformations of the surface elements.

The issue of the initial fixing of the model during manufacture was and remains one of the most relevant ones [2]. Usually, even incomplete exfoliation of the initial laying of a model leads to a change of shape and typically ends with the refusal of the workpiece. That is why the choice of the initial fixation of objects is the basis for reliable reproduction, especially parts that require considerable time for prototyping.

The power supply stability and the absence of network interference and perturbations also directly affect the quality and reliability of printing. It is established that quite often it is the disturbance within a network, as well as a sharp voltage drop, that causes certain disruptions in the printing process and leads to the skipping of the steps of drive engines.

Another important conclusion is the assertion that it is impossible to simply copy the shape of products made from metal by the means of 3-D printing. Since laying the material is quite a complex thermal process, depending on many factors, the finished product can have significant thermal residual stresses. Such stresses are also affected by the amount of extruded plastic; a deviation even in the fraction of the percentage when printing products weighing more than 50 g can lead to significant irreversible deformations of the product. As a result, the product is exfoliated from the base: the normal course of the technological process is disrupted. Exfoliation leads not only to defects in the shape but also to changes in the laying conditions, hence the strength begins to decrease significantly and the finished product has a lower density.

It is shown that such defects are eliminated by the introduction of special ballast elements, which, after processing, are mechanically removed (Fig. 9). However, eliminating the shortcomings of exfoliation does not change the stresses that remain in the finished product after printing.

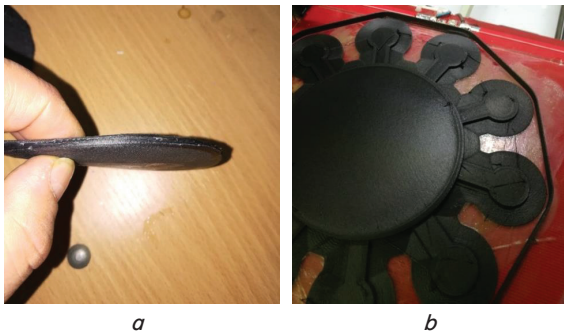

a *b*

Fig. 9. Printed samples:
a — a deformed flat part, obtained without the means of compensation for the stress (a 100 % filling); *b* — a suitable part with compensating elements on the printer table

After mechanical tests and loading the samples to complete destruction, it became apparent that, in general, the cracks formed during destruction are inherent in certain printing conditions. The first is the crack of the normal detachment; there is a stretching of the plane with a crack (Fig. 10, *a*); this type of problem corresponds to the delamination of the material in the plane of adhesion. The second is the crack of the transverse shear; there is an incision in the shear field (Fig. 10, *b*); this type of problem corresponds to the pure shift of the layers, including due to the thermal stresses. The third is a crack of longitudinal shear arising from the deformation of the plate (Fig. 10. *c*).

Therefore, PEEK materials, as well as the reinforced PLA, show the quasi-fragile properties and, under certain conditions, their behavior can be described by the classical theory of the mechanics of the destruction of an elastic body.

Based on our results of testing the mechanical characteristics of the samples, we proceeded to the printing of the flange.

The printing involved two printers simultaneously, the types of Delta and MaketBot. The stages in flange reproduction and the finished flange are shown in Fig. 11.

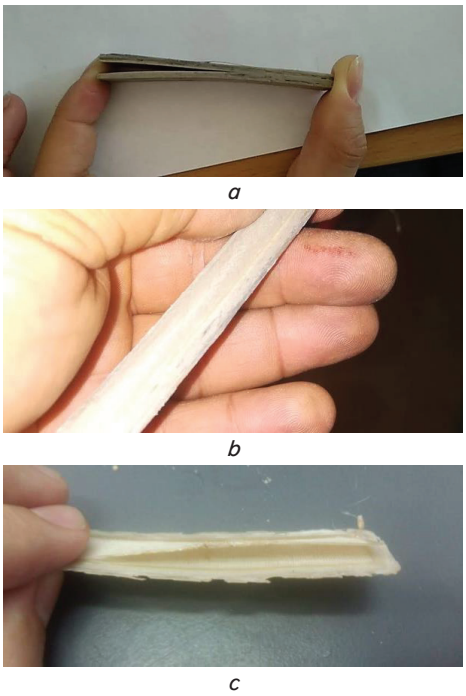

a

b

c

Fig. 10. Examples of the samples for testing the destruction during: *a* — normal loading; *b* — longitudinal movement; *c* — transverse movement

Fig. 11. Stages in flange reproduction and the obtained experimental samples

After receiving satisfactory test results, several working flange samples were produced, which were subsequently subjected to mechanical testing by loading with a working pressure of 1.2 MPa. Of the four flanges printed, two met the technical conditions, having almost the same weight and mechanical properties; one of the products had a higher roughness, but the deviation from the specified size did not exceed 0.7 %.

The flanges were tested in a vacuum chamber. The controlled element is a ring edge ∅135.0–138.5 mm, with a belt width of 9.5 mm (Fig. 12). As a result, the following was established. Test temperature plays a significant role in the gas permeability of the product. Gas permeation is several orders of magnitude less at the temperatures of 20–60 °C and increases rapidly at a temperature above the glassing temperature of the plastic (in our case, 120 °C).

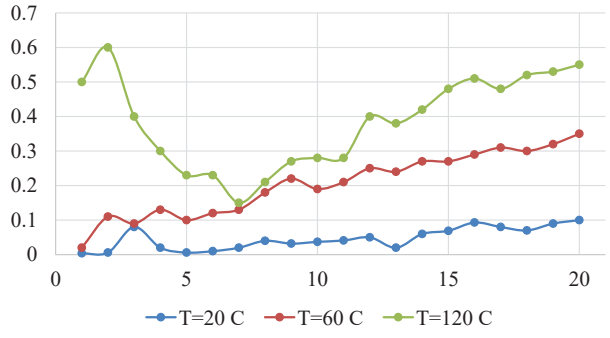

Fig. 12. A change in the vacuum level (P_{init}, Pa) when testing samples from the moment of achieving the residual pressure in the chamber of 10^{-3} Pa (time in min)

Gas permeation is not permanent and increases over time. The increase occurs cyclically and, apparently, approaches critical values over a certain period (about 20 minutes).

To establish the conditions for destruction and determine the critical stresses, the flange is installed in a special device and clamped with a sealed cover; 8 motion sensors are installed in circumference (accuracy of the controlled value is up to 0.01 mm). It was established that the drop in pressure during the test of the round sample from the level of 0.5 MPa was not more than 0.12 % during the tests; the surface of the sample did not demonstrate the air bubbles (of the working environment). Thus, it can be stated that the printed products with a filling of 90 % of the middle and 100 % of the contour do not have significant leakage.

The sensors were connected by a bridge circuit, allowing the most accurate estimate of the movement. The sensors were located on opposite sides of the diameter.

Loading under pressure was above the critical value, changing the pressure from 0.2 MPa to 1.4 MPa. At each pressure level, the flange was left for 1 hour for relaxation. When the pressure increased over 1.2 MPa, the integrity of the product was lost and it was destroyed (Fig. 13, *a*). Its destruction was accompanied by the consistent emergence of the crack and its subsequent asymmetrical opening. Based on the parameters of the material's strength, the destruction should occur when the pressure reaches 1.8–2.0 MPa, which corresponds to the stresses on critical areas at a normal load of 45–55 MPa (Fig. 13, *b*). However, the actual pattern was as follows: when laying the filament (Fig. 4, *a*), the destruction of the sample occurred at a normal load of 34–39 MPa, and when laying (Fig. 4, *b*) – 28–30 MPa. Closest to the expected indicators was a sample with the orthotropic laying (Fig. 4, *c*), which was destroyed under a pressure of 1.67–1.72 MPa (accordingly, at σ=44–48 MPa).

Accordingly, expression (9) can satisfactorily describe the phenomenon of integrity loss only for the orthotropic filament laying, especially for the flange PEEK material; therefore, equations (12), (13) can be used to analyze the behavior of the material. This reasoning also confirms the character of the destruction of the samples shown in Fig. 13, *a*. Thus, we note that under certain conditions of loading the destruction of the examined sample occurs due to the development of normal cracks of separation, transverse, and longitudinal shears.

Consequently, from a practical point of view, ensuring stable characteristics of the interthread adhesion is an important parameter for obtaining maximum strength characteristics. At the same time, the anisotropy of properties allows us to make an assumption about ensuring maximum indicators σ and τ by optimizing the scheme of the filament laying.

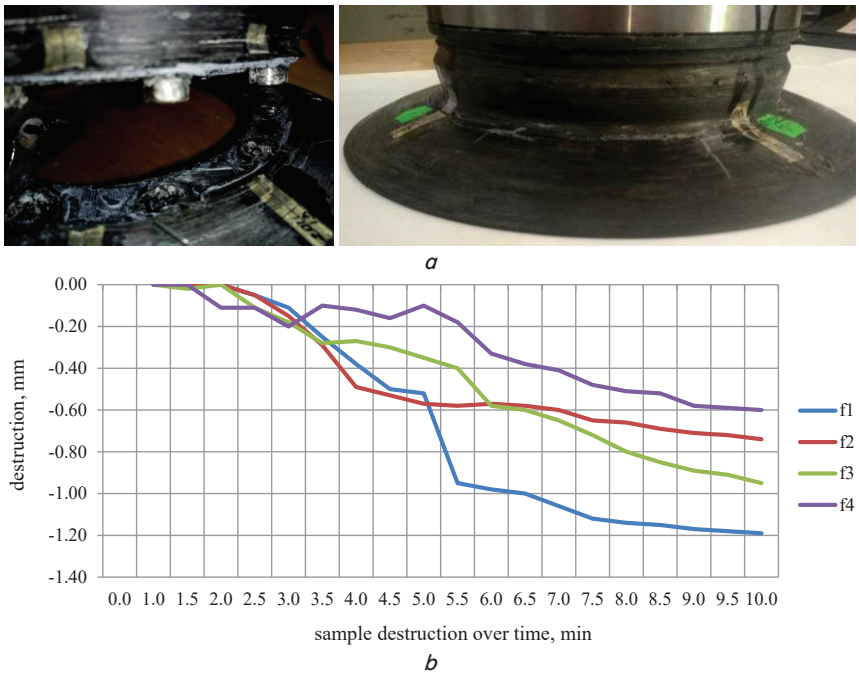

Fig. 13. Flange destruction:
a — during the test; *b* — diagram of moving some elements during testing

when heated, a cavity with oversaturated steam. The cavity stays closed as a result of the action of pressure from the filament, which is fed to the hot zone and the nozzle that forms the molten plastic.

Next, after extruding, the external pressure drops dramatically and the cavity begins to grow, simultaneously with the cooling of the plastic and the reduction of its viscosity (thickening). If during cooling the cavity increases above the critical size, there will be a break of it with the characteristic collapsing sound, which accompanies the printing process. That is when there is a gap at the boundary of an adhesive grip, that is, on the surface, which has a maximum temperature gradient. This is how a micro-break is formed, which is no longer filled with plastic; the subsequent laying of the layers increases tangent stresses and further weakens the surface of adhesion.

The obvious conclusion is that moisture will determine the gas permeability of the product because open cavities (micro-breaks) reduce the resistance to gas leakage.

7. Discussion of results of studying the possibility of ensuring functional properties of the elements and products received by FDM processes

The process of printing responsible parts is quite time-consuming and resource-intensive. This study allowed us to establish a significant number of limitations and features in the implementation of the process, which are directly related to the indicators of quality and reproducibility of the mechanical characteristics of the product, as well as its functional properties.

In particular, it is problematic to predict the stressed-deformed state of products based on the classical theories of the deformed body mechanics, taking into consideration the size of the nucleated cracks (or initial defects) l and the stresses established from (11).

Even in the absence of embedded elements (Fig. 9), the emerging radial cracks open at stresses σ_x, σ_y, τ_{xy}, which are 0.75–0.8 $[\sigma]$ and 0.55–0.62 $[\tau]$. This is evidenced by the actual test results (Fig. 12) for a time of more than 2 s, as well as differences in the achieved strength of the samples with different types of laying (Fig. 4). Consequently, patterns (11), (12), and (17) require clarification for the different types of filament laying.

A rather wide range of spread of the controlled (and, consequently, estimation values) can be explained by certain perturbations in the process when full control over printing cannot be achieved. Moreover, the more complex the part, the worse the control, and the greater the initial deviations in the printing processes.

Thus, in particular, it is shown that the mechanical characteristics of the product are affected by the moisture content of the material, as well as the temperature phenomena after extruding the plastic. At the same time, humidity requirements for PEEK plastic are more stringent than for the reinforced PLA plastic. For the latter, the presence of moisture causes the emergence of zones of internal defects in the form of cavities. The mechanism of their formation can be explained by the accumulation, on the surface of the multimolecular layer, of water, which forms,

Regarding the results shown in Fig. 12, it should be noted that certain cyclical changes in gas permeability can be explained by gradual temperature changes in the structure of the plastic. This conclusion is also prompted by the comparison of gas permeation at different temperatures. Thus, at T=20 °C, the gas permeability grows slower than at T=60 °C and T=120 °C.

The geometric parameters of the product, especially when printing at high temperatures (over 400 °C), had a significant spread. Thus, it was established that for sizes of 150–200 mm, the spread can mount to 0.24–0.45 mm, which corresponds to IT9–IT10 and worse. Consequently, additional machining is required, which, simultaneously with the improvement of the quality of the surface layer (reducing its roughness), can significantly reduce the area of a 100 % fill.

Thus, ensuring the functional properties of responsible products obtained using 3-D printing from structural polymeric reinforced materials implies the development of a system of techniques and methods for laying the plastic using conventional extrusion heads. Accordingly, it is necessary to cover the issue of determining the shape of a product, the presence of compensators, and the choice of appropriate plastic.

Further research should be aimed at establishing patterns of strength characteristics depending on different obtaining methods, the laying of layers, and using certain additives to the filament. To be additionally studied is the possibility of transition from the plane laying to laying on rotary tables, which could form a cylindrical shape of products more reliably.

8. Conclusions

1. We have established patterns of the effect exerted by the 3-D printing conditions on achievable roughness (at the level of 6.3 μm) and accuracy of size execution corresponding to the IT9–IT10 quality. Temperature deformations have been defined (for PEEK-Carbon ~0.6–0.8 %). The dependence of the emergence of defects in the form of exfoliation and adhesion

reduction on the laying scheme of the extruded material (extrusion coefficient, filling, layer thickness) has been shown.

2. It has been determined that the reduction of the strength of the finished product is caused not only by reducing the contact of adhesion but also by manifestations of the phenomena of crack formation when critical stresses from workloads are achieved. These stresses are the greater the smaller the contact area between the layers. Experimentally, it has been proven that the destruction of the printed flange made from the PEEK material occurs at a pressure of 1.2 MPa, which corresponds to stresses on critical areas with a normal load of 30–35 MPa. There is a conditionality of the critical loading by a filament laying technique; the maximum indicators are provided at orthotropic laying.

3. The patterns of gas permeability of printed products have been established and it is shown that the permeability depends on the temperature and increases rapidly with the temperature approaching the level of glassing of the plastic (base). For PLA+Carbon, this temperature is 120 °C.

4. It has been concluded that ensuring the functional properties of responsible products implies the simultaneous implementation of the structural improvements of the product with the introduction of additional compensating elements (which are subsequently removed). In addition, an important factor is the orthotropic laying of filament with the minimization of external influences on the process of extrusion and cooling.

References

1. Xu, Y., Deng, C. (2017). An investigation on 3D printing technology for power electronic converters. 2017 IEEE 8th International Symposium on Power Electronics for Distributed Generation Systems (PEDG). doi: https://doi.org/10.1109/pedg.2017.7972486
2. Shahrubudin, N., Lee, T. C., Ramlan, R. (2019). An Overview on 3D Printing Technology: Technological, Materials, and Applications. Procedia Manufacturing, 35, 1286–1296. doi: https://doi.org/10.1016/j.promfg.2019.06.089
3. Wang, X., Jiang, M., Zhou, Z., Gou, J., Hui, D. (2017). 3D printing of polymer matrix composites: A review and prospective. Composites Part B: Engineering, 110, 442–458. doi: https://doi.org/10.1016/j.compositesb.2016.11.034
4. Joshi, S. C., Sheikh, A. A. (2015). 3D printing in aerospace and its long-term sustainability. Virtual and Physical Prototyping, 10 (4), 175–185. doi: https://doi.org/10.1080/17452759.2015.1111519
5. Wang, Y., Blache, R., Xu, X. (2017). Selection of additive manufacturing processes. Rapid Prototyping Journal, 23 (2), 434–447. doi: https://doi.org/10.1108/rpj-09-2015-0123
6. Samykano, M., Selvamani, S. K., Kadirgama, K., Ngui, W. K., Kanagaraj, G., Sudhakar, K. (2019). Mechanical property of FDM printed ABS: influence of printing parameters. The International Journal of Advanced Manufacturing Technology, 102 (9-12), 2779–2796. doi: https://doi.org/10.1007/s00170-019-03313-0
7. Dizon, J. R. C., Espera, A. H., Chen, Q., Advincula, R. C. (2018). Mechanical characterization of 3D-printed polymers. Additive Manufacturing, 20, 44–67. doi: https://doi.org/10.1016/j.addma.2017.12.002
8. Caminero, M. A., Chacón, J. M., García-Moreno, I., Rodríguez, G. P. (2018). Impact damage resistance of 3D printed continuous fibre reinforced thermoplastic composites using fused deposition modelling. Composites Part B: Engineering, 148, 93–103. doi: https://doi.org/10.1016/j.compositesb.2018.04.054
9. Gardan, J., Makke, A., Recho, N. (2016). A Method to Improve the Fracture Toughness Using 3D Printing by Extrusion Deposition. Procedia Structural Integrity, 2, 144–151. doi: https://doi.org/10.1016/j.prostr.2016.06.019
10. Baumann, F., Bugdayci, H., Grunert, J., Keller, F., Roller, D. (2015). Influence of slicing tools on quality of 3D printed parts. Computer-Aided Design and Applications, 13 (1), 14–31. doi: https://doi.org/10.1080/16864360.2015.1059184
11. Keleş, Ö., Blevins, C. W., Bowman, K. J. (2017). Effect of build orientation on the mechanical reliability of 3D printed ABS. Rapid Prototyping Journal, 23 (2), 320–328. doi: https://doi.org/10.1108/rpj-09-2015-0122
12. Yang, Y. F., Tang, C. A., Xia, K. W. (2012). Study on crack curving and branching mechanism in quasi-brittle materials under dynamic biaxial loading. International Journal of Fracture, 177 (1), 53–72. doi: https://doi.org/10.1007/s10704-012-9755-6
13. Ma, G., Dong, Q., Wang, L. (2018). Experimental investigation on the cracking behavior of 3D printed kinked fissure. Science China Technological Sciences, 61 (12), 1872–1881. doi: https://doi.org/10.1007/s11431-017-9192-7
14. Zeng, Q., Tonge, A. L., Ramesh, K. T. (2019). A multi-mechanism constitutive model for the dynamic failure of quasi-brittle materials. Part I: Amorphization as a failure mode. Journal of the Mechanics and Physics of Solids, 130, 370–392. doi: https://doi.org/10.1016/j.jmps.2019.06.012
15. Zeng, Q., Tonge, A. L., Ramesh, K. T. (2019). A multi-mechanism constitutive model for the dynamic failure of quasi-brittle materials. Part II: Integrative model. Journal of the Mechanics and Physics of Solids, 131, 20–42. doi: https://doi.org/10.1016/j.jmps.2019.06.015
16. Salenko, A., Chencheva, O., Lashko, E., Shchetynin, V., Klimenko, S., Samusenko, A. et. al. (2018). Forming a defective surface layer when cutting parts made from carbon-carbon and carbon-polymeric composites. Eastern-European Journal of Enterprise Technologies, 4 (1 (94)), 61–72. doi: https://doi.org/10.15587/1729-4061.2018.139556
17. Salenko, A., Chencheva, O., Glukhova, V., Shchetynin, V., Budar, M. R. F., Klimenko, S., Lashko, E. (2020). Effect of slime and dust emission on micro-cutting when processing carbon-carbon composites. Eastern-European Journal of Enterprise Technologies, 3 (1 (105)), 38–51. doi: https://doi.org/10.15587/1729-4061.2020.203279
18. Dragobetskii, V., Zagirnyak, V., Shlyk, S., Shapoval, A. Naumova, O. (2019). Application of explosion treatment methods for production Items of powder materials. Przegląd elektrotechniczny, 1 (5), 41–44. doi: https://doi.org/10.15199/48.2019.05.10